Progress In Electromagnetics Research, Vol. 152, 127–136, 2015

Adaptive Transmission Method for Alleviating the Radio Blackout Problem

Guolong He[1, 2, *], Yafeng Zhan[1], and Ning Ge[1]

Abstract—The radio blackout problem stands as one long obstacle for hypersonic flight and planetary atmosphere reentry. Rather than previous physical mitigation methods aiming to reduce the plasma electron density, this paper proposes a novel method which attempts to communicate at carrier frequency much higher than the plasma cutoff frequency. To overcome the highly dynamic channel characteristics, the reflected wave is used online to estimate the instantaneous channel states and enable adaptive transmission. According to the predicted channel states, the plasma sheath induced phase shift and amplitude attenuation are compensated by baseband modulation and power adaptation, respectively. Numerical simulations are presented and discussed, in order to illustrate the effectiveness of the proposed method.

1. INTRODUCTION

When a vehicle flies at hypersonic velocity or a spacecraft enters into planetary atmosphere, the tremendous heat converted from atmospheric friction will cause dissociation and ionization of surrounding air molecules, resulting in the formation of the so-called "plasma sheath". Under such circumstances, all the communication, navigation and telemetry signals will be disrupted or at least severely degraded, leading to the well-known "radio blackout" problem [1–6].

Since the era of the Apollo program, this problem has attracted much attention over the past decades [1–14]. The effects of the plasma sheath can generally be divided into two aspects. As shown in Fig. 1, the static attenuation caused by plasma sheath first increases then decreases with the increasing electromagnetic wave transmission frequency, where the most severe condition occurs near the plasma cutoff frequency f_p,

$$f_p = \frac{1}{2\pi}\sqrt{\frac{n_e e^2}{\varepsilon_0 m_e}} \tag{1}$$

where n_e is the electron density, $e = 1.6022 \times 10^{-19}$ C the electron charge, $m_e = 9.1 \times 10^{-31}$ kg the electron mass, and $\epsilon_0 = 8.8542 \times 10^{-12}$ F/m the permittivity in free space.

It's certainly feasible to alleviate the radio blackout problem if one can reduce the plasma electron density. Many physical mitigation methods were proposed from this point of view, and some of them have already shown their potential, e.g., aerodynamic shaping [7], liquid quenchant injection [8], resonant transmission [9], inflatable aeroshell [10], and electromagnetic windowing [11]; see [14] for a very good summary. However, all the proposals have their own practical shortages or engineering obstacles. No satisfactory solution has yet been proven, leaving this problem still unsolved.

Another probably feasible solution is to communicate at frequency much higher than the plasma cutoff frequency. For the entry, descent, and landing (EDL) stage of recent NASA Mars exploration

Received 27 July 2015, Accepted 25 August 2015, Scheduled 30 August 2015

* Corresponding author: Guolong He (heguolong@alumni.sjtu.edu.cn).

[1] Space Centre, Tsinghua University, Beijing 100084, China. [2] Beijing Institute of Tracking and Telecommunication Technology, Beijing 100094, China.

missions, both the rover aerodynamic performance and landing trajectory are carefully designed to make the ionized electron density and the corresponding plasma cutoff frequency as low as possible. Two communication links with much higher carrier frequencies are simultaneously established, one UHF-band link for orbiter relay and the other X-band link for direct-to-Earth (DTE) communication [15–18]. Rather than conventional phase-coherent communication scheme, a special form of M-ary Frequency Shift Keying (MFSK) modulation is used to transmit one out of 256 data tones every 10 seconds over the DTE link [16, 17]. The primary concern for such design is that huge channel dynamics would easily cause communication failure at such high frequency. Carrier estimation and data detection are also very challenging under such low signal-to-noise ratio (SNR) levels and highly dynamical conditions. The current carrier recovery procedure is based on open loop architecture and maximum likelihood (ML) technique [18]. Some efforts have been made to improve the communication system reliability under this critical stage. A novel approach that takes into account the power of data tones was proposed in [19] to enhance carrier recovery performance by up to 3 dB. Lopes et al. also designed a robust and low complexity scheme consisting of a bank of adaptive linear predictors supervised by a convex combiner to estimate and track the carrier frequency combined with some additional enhancement techniques [20]. All these aforementioned efforts were made at the receiver side.

In this paper, we propose a totally different idea which works at the transmitter side only. The strong reflected wave from the plasma sheath is used to enable adaptive transmission. However, we restrict our discussion to only focus on the effects of the plasma sheath, and not include other factors such as rover deceleration, parachute deployment induced antenna pointing angle variation, and extreme Doppler dynamics. The remainder of this paper is organized as follows. First, the basic principle of adaptive transmission method is introduced in Section 2. Then Section 3 presents the implementation details of channel prediction technique along with adaptive transmission strategy. Some numerical simulations are presented to demonstrate the effectiveness of the proposed method in Section 4. Finally, this paper is summarized and concluded in Section 5.

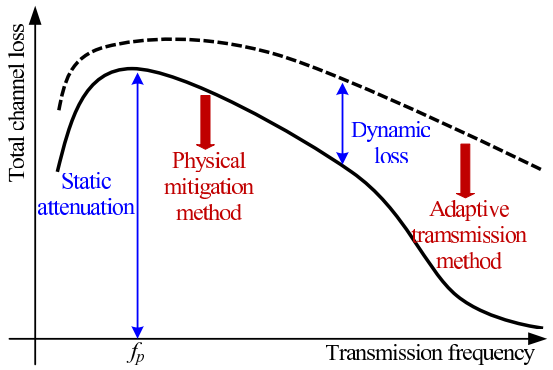

Figure 1. The static (solid line) and dynamic (dash line) effects of the plasma sheath and the corresponding possible alleviating methods.

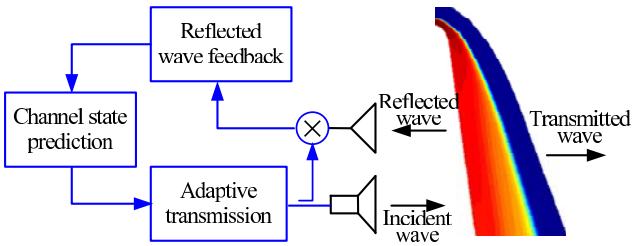

Figure 2. Block diagram of the adaptive transmission method.

2. ADAPTIVE TRANSMISSION METHOD

In conventional wireless communication, the channel characteristics are affected by reflection and scattering of open environment, causing multipath effects and fading phenomenon. The transmitter does not know the channel conditions unless the receiver feeds back this information. Unfortunately, very little energy from the electromagnetic wave can penetrate the plasma sheath and be received by the ground station. Hence, it's usually too weak for normal detection under this scenario and the corresponding channel characteristics cannot be measured and fed back effectively.

Luckily, we do not need to seek far away and neglect what lies close at hand. In the radio blackout problem, the channel variations are mainly induced by plasma electron density variations, which also has an impact on the reflected wave. Fig. 2 illustrates the general idea of the adaptive transmission method

for alleviating this problem. Since the incident wave is reflected to the spacecraft without path loss, we can online measure the instantaneous channel states from the reflected wave indirectly. Although the obtained channel characteristics are imperfect, they can be further utilized for channel prediction and adaptive transmission.

The idea of adaptive transmission is well known for wireless communication [21–26]. The basic premise is to instantaneously estimate the time-varying channel states at the receiver and feed it back to the transmitter, so that the transmission scheme can be adapted in response to channel variations [21–23]. This is rather different from the traditional nonadaptive design, where the link margin is pre-determined according to the worst case to maintain acceptable performance and ensure reliable communication over the whole event. However, there are some obvious differences in the radio blackout problem. First, traditional adaptive transmission require feedback from the receiver, which always suffers a long time delay and some quantization errors. For the plasma sheath scenario, the channel state information just comes from the reflected wave, a relatively much shorter time delay is expected but the estimated channel states are imperfect. Second, many adaptation methods have been proposed for wireless communication. However, some of them are not suitable for practical space communication, so we should select an efficient and also suitable adaptation strategy and keep it as simple as possible. Moreover, it's usually assumed that the phase-locked loop (PLL) can perfectly track the carrier phase for wireless communication. In the radio blackout problem, however, the phase variation caused by the plasma sheath must be taken into account due to its highly dynamic characteristics.

3. SYSTEM MODEL AND ALGORITHM IMPLEMENTATION

3.1. Plasma Sheath Channel Model

As the electromagnetic wave interacts with the plasma sheath, the wave energy is transmitted, reflected and absorbed, which obeys the Maxwell's equations,

$$\begin{aligned} \nabla \times \mathbf{E} &= -j\omega\mu_0 \mathbf{H} \\ \nabla \times \mathbf{H} &= j\omega\epsilon_0\epsilon_r(\omega)\mathbf{E} \end{aligned} \tag{2}$$

where $\omega = 2\pi f$ is the wave transmission frequency, $\mu_0 = 4\pi \times 10^{-7}\,\mathrm{H/m}$ the permeability in free space, and the relative permittivity of plasma $\epsilon_r(w)$ has the following expression,

$$\epsilon_r(\omega) = 1 - \frac{\omega_p^2}{\omega^2 - j\omega v_p} \tag{3}$$

where $\omega_p = 2\pi f_p$ is the plasma cutoff frequency in radians, and v_p is the plasma collision frequency. Since the plasma electron density varies with time, ω_p and ϵ_r and the electric and magnetic fields are also time-variant. The collision frequency v_p at high-temperature air is estimated by the following empirical expression [4, 27],

$$v_p = 3 \times 10^8 \frac{\rho}{\rho_0} T_p \tag{4}$$

where ρ/ρ_0 ($\rho_0 = 1.288\,\mathrm{kg/m^3}$) is the air density ratio and T_p the local temperature in Kelvin. The transmission and reflection coefficients, T and R, can be generally expressed as [28, 29],

$$\begin{aligned} T(t) &= f_T(n_e) + w_T(t) \\ R(t) &= f_R(n_e) + w_R(t) \end{aligned} \tag{5}$$

where f_T and f_R are functions that are nonlinear with the plasma electron density, both of which have no closed-form expressions and must be determined numerically under the boundary continuity conditions of tangential fields [29]. The variables $w_T(t)$ and $w_R(t)$ are uncorrelated disturbances which are usually modeled as white Gaussian random processes. To indicate the relative weights between these two parts, the correlation coefficient Ω is defined as follows,

$$\Omega = \sigma_w/\sigma_f \tag{6}$$

where σ_f and σ_w are the standard variances of the plasma electron density induced dynamic and uncorrelated disturbance, respectively. For $\Omega_T = \Omega_R = 0$, T and R are highly correlated, thus we

can expect a well adaptation performance; while for Ω_T or $\Omega_R = \infty$, they are totally independent and adaptation is meaningless in this case.

As can be seen in Eq. (5), in order to simulate the time-varying transmission and reflection coefficients, first the electron density variation must be generated. A few ground test experiments have been conducted to investigate the electron density turbulence intensity of the plasma sheath [30]. Unfortunately, all of their data give only qualitative rather than quantitative information. Here we adopt the Demetriades's model obtained from Jet Propagation Laboratory (JPL) hypersonic wind tunnel measurement data [31, 32]. The power spectral density (PSD) $S_n(f)$ is assumed to be pink-colored and dominant in the low frequency region, while a '$-5/3$' Kolmogorov decay is observed at high frequencies, i.e., $S_n(f) \sim f^{-5/3}$. Hence, the time-varying electron density $n_e(x,t)$ is modeled as,

$$n_e(x,t) = n_{ss}(x) \times [1 + \Delta \cdot n(t)] \tag{7}$$

where $n_{ss}(x)$ is the steady-state plasma electron density spatial distribution, Δ the relative turbulence intensity, and $n(t)$ a non-stationary colored Gaussian noise process with unit standard deviation.

3.2. Channel State Prediction

No matter how fast the reflected wave can be sampled and fed back, the estimated channel states are still outdated and not sufficient at the time of transmission. To realize the potential of adaptive transmission, the channel characteristics need to be known ahead. Usually, future transmitted channel state can be predicted by the autoregressive (AR) model,

$$\hat{T}(nT_s) = \sum_{k=1}^{p} c_k \times R\left((n-k)T_s\right) \tag{8}$$

where p is the AR model order, T_s the sampling time interval, and $R((n-k)T_s)$ are previous reflected channel state samples. The coefficients c_k can be determined by using the minimum mean square error (MMSE) criterion [24–26],

$$\mathbf{c} = \mathbf{Q}^{-1}\mathbf{d} \tag{9}$$

where $\mathbf{c} = [c_1\ c_2\ \ldots\ c_p]^T$, $\mathbf{Q}$ is the $p \times p$ autocorrelation matrix with $Q_{ij} = E\{R^*((n-i)T_s)R((n-j)T_s)\}$, and $\mathbf{d}$ is the $p \times 1$ cross-correlation vector with $d_i = E\{R^*((n-i)T_s)T(nT_s)\}$. Eq. (8) is also referred as one-step linear predictor or the Yule-Walker equations, whose coefficients can be efficiently calculated by Levinson-Durbin recursion [26].

3.3. Adaptation Transmission Strategy

Adaptive transmission refers to adapt some strategies of constellation size, symbol rate, coding scheme, transmitted power, antenna diversity, or any combination of these parameters [23]. However, as mentioned earlier, some of them are not suitable for space communication. For example, fixed-rate transmission with real-time delay constraints is much preferred for voice and telemetry transmission rather than variable-rate transmission. This suggests that it's more favorable to adopt fixed-rate transmission combined with power adaptation, where the transmitter adjusts its power to maintain a relative constant signal level at the receiver. Hence, the traditional Binary Phase Shift Keying (BPSK) modulation is adopted in this work, because of its wide usage for space communication. We first compensate the predicted phase shift caused by plasma sheath during the modulation stage,

$$\theta(nT_s) = \pm\pi - \angle\hat{T}(nT_s) \tag{10}$$

where $+\pi$ means sending bit '1', while $-\pi$ means sending bit '0'.

We then adapt the transmitted power P_t according to the predicted transmission attenuation of the plasma sheath,

$$P_t(nT_s) = KP_{av}\left|\hat{T}(nT_s)\right|^2 \tag{11}$$

where P_{av} is the average transmitted power, and K is a scalar determined by the power constraint,

$$P_{av} = E\left\{P_t\right\} = \int P_t \cdot p(T)dT \tag{12}$$

where $p(T)$ is the probability density function (PDF) of the transmission coefficient. By substituting (11) into (12), we can obtain that

$$K = 1 \Big/ \int |T|^2 p(T) dT \tag{13}$$

Here we do not employ the cutoff SNR scheme to improve the average spectral efficiency as in Chapter 9 of Ref. [22], which would induce an outage probability.

4. NUMERICAL SIMULATION

In this section, we present some numerical simulations and their results to demonstrate the benefit of our proposed method. Fig. 3 illustrates the simulation flowchart with the main steps. We assume that the transmitted and reflected waves have the same correlation coefficient in the simulation, i.e., $\Omega_T = \Omega_R = \Omega$. First, we use computational fluid dynamics (CFD) technique to obtain the steady-state plasma sheath distribution of a Radio Attenuation Measurements (RAM) project blunt model [2]. The thermochemical nonequilibrium problem is solved based on Navier-Stokes equations, employed with an eleven-species air-reacting chemistry model [32]. Key parameters for CFD simulation are summarized and presented in Table 1. As can be seen in Fig. 4, the air around the vehicle is compressed and a shock wave is formed. The onboard antenna is mounted in the rear region of the blunt body, which has a significantly lower plasma electron density and much less influence of the plasma sheath than other areas.

The plasma electron density profile radially outward from the onboard antenna is extracted as the steady-state distribution. With very low computational complexity and high efficiency, the transmission matrix method is used to numerically investigate the impact of plasma electron density variation on electromagnetic wave propagation (see the Appendix for algorithm implementation details). Fig. 6 illustrates the steady-state amplitude attenuation and phase shift of the reentry plasma sheath. One can see that the transmission coefficient first decreases then increases with the increasing frequency, which has a peak attenuation of approximately -70 dB near X-band (8.4 GHz). This is because that the peak

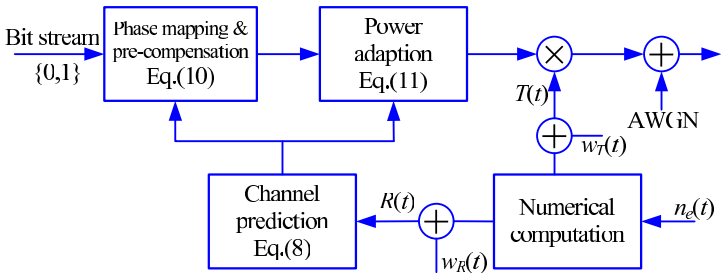

Figure 3. The numerical simulation flowchart of adaptive transmission method.

Table 1. Key parameters for CFD simulation.

Type	Parameters	Numerical value
Blunt configuration	Blunt length	1 m
	Nose radius	0.1 m
	Half cone angle	10°
	Antenna location	(0.814 m, 0.243 m)
Flight attitude	Velocity	6 km/s
	Angle of attack	0°
Atmosphere condition	Static temperature	270 K
	Static pressure	80 Pa

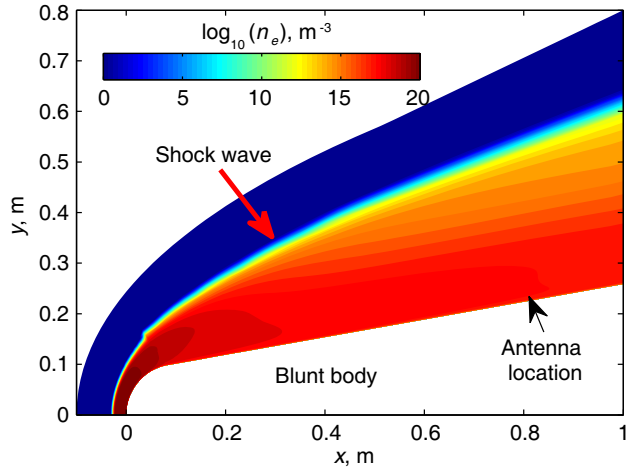

Figure 4. The steady-state electron density distribution obtained from CFD simulation, with blunt velocity of 6 km/s.

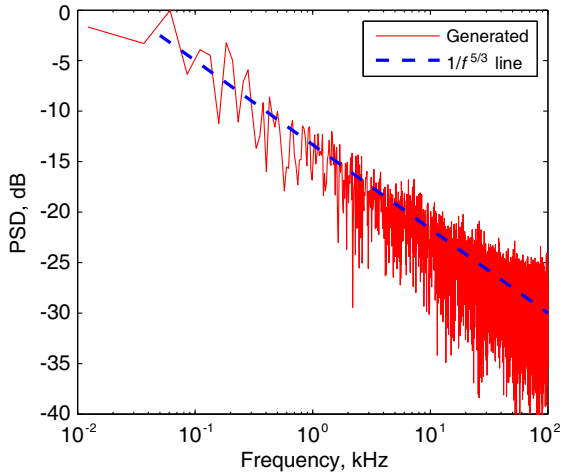

Figure 5. The PSD of the generated colored noise process.

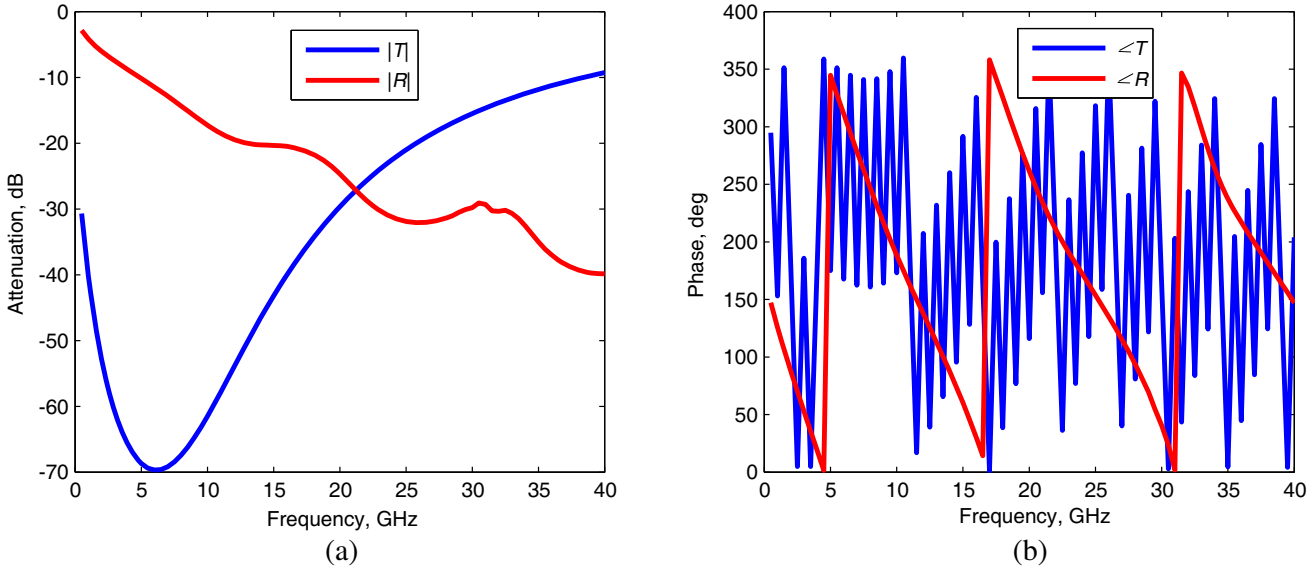

Figure 6. The steady-state influences of the reentry plasma sheath. (a) Amplitude attenuation. (b) Phase shift.

plasma electron density is on the order of $10^{18}\,\mathrm{m}^{-3}$, which corresponds to the maximum plasma cutoff frequency $f_p \sim 9\,\mathrm{GHz}$. Hence, we consider Ka-band (32 GHz) for possible communication, where the transmission attenuation is relative less, and the reflection coefficient is still high enough for reflected wave feedback. (The transmission frequency selection should obey some standards to meet onboard system requirements, Ka-band is recommended by CCSDS and widely adopted by some recent space missions.)

The non-stationary $f^{-5/3}$ colored Gaussian noise process is generated by a 200-order discrete infinite impulse response (IIR) filter [33], whose PSD is illustrated in Fig. 5. Fig. 7 presents an example of the amplitude variation and phase fluctuation of Ka-band transmitted and received waves with sampling frequency of 200 kHz. At such high carrier frequency, the magnitudes of the transmission and reflection coefficients are approximately $-15\,\mathrm{dB}$ and $-30\,\mathrm{dB}$, respectively. Compared to conventional low frequency transmission near or under the plasma cutoff frequency, the relative less amplitude attenuation

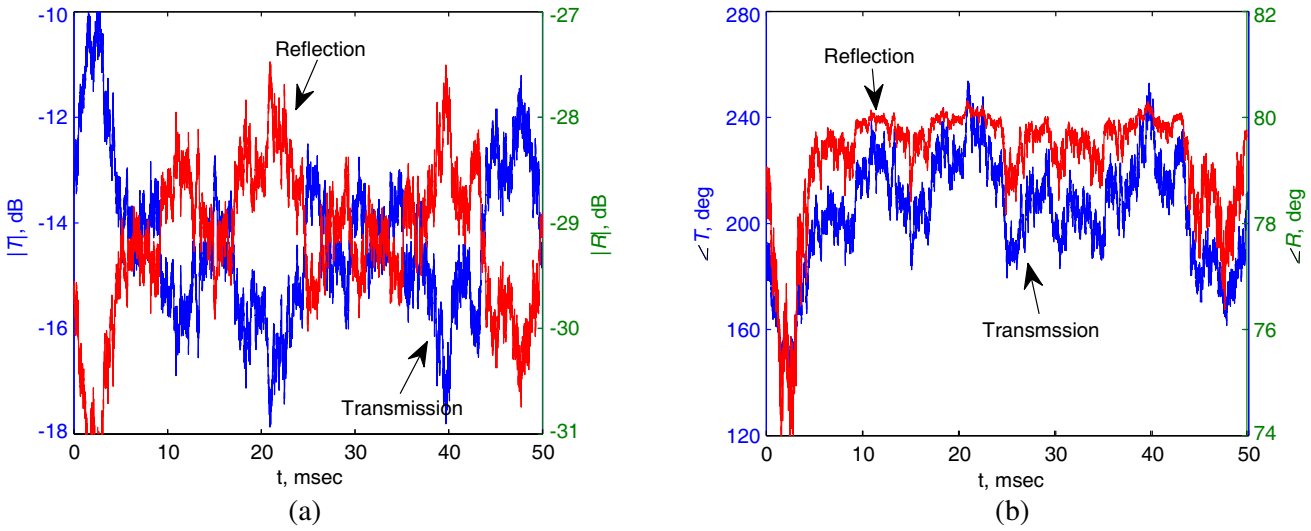

Figure 7. Typical time variations of the Ka-band transmitted and reflected waves with $\Delta = 10\%$ and $\Omega = 0.1$. (a) Amplitude variation. (b) Phase fluctuation.

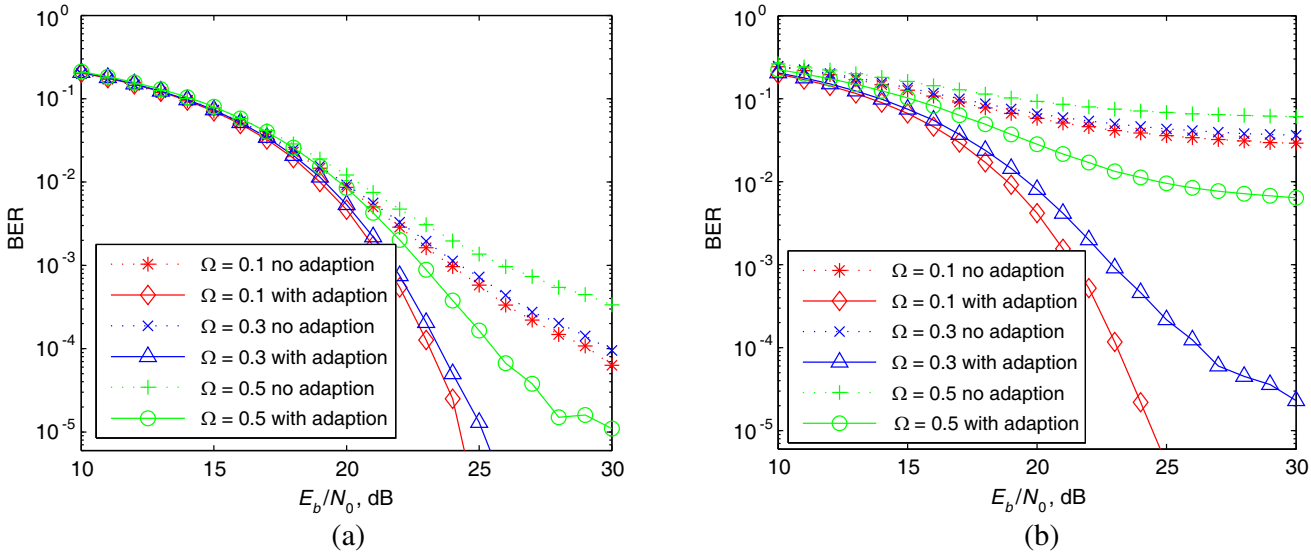

Figure 8. Performance comparisons for adaptive and nonadaptive transmissions. (a) $\Delta = 10\%$. (b) $\Delta = 20\%$.

makes communicate with the ground station possible. Since the reflected wave is directly sampled by the onboard antenna without any path loss, the obtained SNR is large enough for sampling and channel estimation. Moreover, the most important thing is that, high correlations between these two waves can be observed from not only amplitude variation but also phase variation. The amplitude variations have very strong negative correlation. One signal increases while the other decreases, and vice versa. By contrast, their phases are positively correlated. These data confirm the feasibility of the proposed method.

Finally, the performance of adaptive transmission is evaluated by Monte Carlo simulations. Without loss of generality, we consider an uncoded communication system. We choose the symbol rate to be the same as the channel sampling frequency and assume the feedback delay of one symbol interval. The AR model order of the channel predictor is set to 50 as recommended by previous literatures [25, 26]. The results obtained for different plasma parameters are given in Fig. 8. For plasma relative turbulence

intensity $\Delta = 10\%$, significant gains (larger than 5 dB for most cases) can be obtained relative to nonadaptive transmission. The performance improvements for $\Delta = 20\%$ are even more evident, where bit error rate (BER) tail phenomena occurs for nonadaptive transmission, while adaptive transmission can still work well under the same condition. However, it should keep in mind that, we haven't added high Doppler dynamics and attitude variation effects in the simulation, thus worse performance with detection and demodulation loss should be expected in practical implementation.

5. CONCLUSION AND FUTURE RESEARCH

This paper proposes a novel adaptive transmission method which works on the transmitter side to alleviate the radio blackout problem. The strong reflected wave from the plasma sheath is used online to measure the instantaneous channel states indirectly, and further utilized for channel prediction and adaptive transmission. According to the predicted channel states, the plasma sheath induced phase shift and amplitude attenuation are compensated by baseband modulation and power adaptation, respectively. Numerical simulations show that, adaptive transmission can obtain more than 5 dB performance gain relative to nonadaptive transmission for most cases.

However, there are still some open research problems which need to be further investigated before practical implementation. First and foremost, due to the difficulty of performing laboratory experiments, expense of test flights and lack of measurement data, there is not a widely accepted plasma sheath electron density variation model. The hypersonic high-temperature gas dynamics and its turbulence mechanism are hot research topics and still not well understood. Currently the empirical non-stationary $f^{-5/3}$ colored Gaussian noise process is used in this work, more accurate channel model may be obtained if we can model the electron density dynamics not only the temporal variation but also the spatial turbulence. Second, to assure the feedback information timely and effective, the whole loop including onboard reflected wave sampling circuit, channel prediction algorithm implementation and signal processing unit should have a total time delay as small as possible and must be carefully calibrated before launch. Besides these, some other adaption schemes, such as constellation adaption and code adaption, are also very attractive and can be combined with the strategy proposed in Section 3.3. To keep focus on the intrinsic objective of this work and match the aims and scope of this journal, we do not expand the discussion here for their high relevance with communication theory. Moreover, additional experiments and in-flight tests are favorable to validate and support the proposed method.

APPENDIX A. TRANSMISSION MATRIX METHOD

Since the electron density distribution of the plasma sheath is nonuniform, numerical methods must be adopted to investigate the interactions between plasma and electromagnetic wave. Here we adopt the transmission matrix method because of its high efficiency and simplicity. We first divide the plasma sheath into N subslabs, each subslab is assumed to be uniform with the wavenumber k_n and the length d_n, $n = 1, 2, \ldots, N$. Defining E_n^+ and E_n^- as the electric fields of the nth subslab with the $+z$ and $-z$ directions, respectively, then they can be expressed as a function of the electric fields of the next subslab in a recursive manner [34],

$$\begin{bmatrix} E_n^+ \\ E_n^- \end{bmatrix} = \frac{1}{1+\rho_n} \begin{bmatrix} e^{jk_n d_n} & \rho_n e^{-jk_n d_n} \\ \rho_n e^{jk_n d_n} & e^{-jk_n d_n} \end{bmatrix} \begin{bmatrix} E_{n+1}^+ \\ E_{n+1}^- \end{bmatrix} \tag{A1}$$

where ρ_n is the reflection coefficient of the interface between the nth and $n+1$th subslabs,

$$\rho_n = \frac{k_n - k_{n+1}}{k_n + k_{n+1}} \tag{A2}$$

For the rightest semi-infinite free space region, there is no reflected electric field and the equation is modified as,

$$\begin{bmatrix} E_N^+ \\ E_N^- \end{bmatrix} = \frac{1}{1+\rho_N} \begin{bmatrix} 1 & \rho_N \\ \rho_N & 1 \end{bmatrix} \begin{bmatrix} E_{N+1}^+ \\ 0 \end{bmatrix} \tag{A3}$$

From the electric fields, the transmission and reflection coefficients of the plasma can be obtained,

$$T = E_{N+1}^+ / E_0^+, \quad R = E_0^- / E_0^+ \tag{A4}$$

ACKNOWLEDGMENT

This work was supported by the National Key Basic Research Program of China (2014CB340206), National Natural Science Foundation of China (61271265 and 61132002), and Tsinghua University Initiative Scientific Research Program (2011Z05112).

REFERENCES

1. Rybak, J. P. and R. J. Churchill, "Progress in reentry communications," *IEEE Transactions on Aerospace and Electronic Systems*, Vol. 7, No. 5, 879–894, Sep. 1971.
2. Akey, N. D., "Overview of RAM reentry measurements program," *The Entry Plasma Sheath and Its Effects on Space Vehicle Electromagnetic Systems*, 19–31, 1970.
3. Morabito, D. D., "The spacecraft communications blackout problem encountered during passage or entry of planetary atmospheres," *IPN Progress Report 42-150*, 1–16, Aug. 2002.
4. Shi, L., B. Guo, Y. Liu, and J. Li, "Characteristic of plasma sheath channel and its effect on communication," *Progress In Electromagnetic Research*, Vol. 123, 321–336, 2012.
5. Bai, B., X. Li, Y. Liu, J. Xu, L. Shi, and K. Xie, "Effects of reentry plasma sheath on the polarization properties of obliquely incident EM waves," *IEEE Transactions on Plasma Science*, Vol. 42, No. 10, 3365–3372, Oct. 2014.
6. Hartunian, R. A., G. E. Stewart, S. D. Fergason, T. J. Curtiss, and R. W. Seibold, "Causes and mitigation of radio frequency (RF) blackout during reentry of reusable launch vehicles," *Contractor Rep. ATR-2007(5309)-1*, Aerospace Corporation, CA, 2007.
7. Belov, I. F., V. Ya. Borovoy, V. A. Gorelov, A. Y. Kireev, A. S. Korolev, and E. A. Stepanov, "Investigation of remote antenna assembly for radio communication with reentry vehicle," *Journal of Spacecraft and Rockets*, Vol. 38, No. 2, 249–256, Mar. 2001.
8. Hinson, W. F., P. B. Gooderum, and D. M. Bushell, "Experimental investigation of multiple-jet liquid injection into hypersonic flow," TN D-5861, NASA, Jun. 1970.
9. Sternberg, N. and A. I. Smolyakov, "Resonant transmission of electromagnetic waves in multilayer dense-plasma structures," *IEEE Transactions on Plasma Science*, Vol. 37, No. 7, 1251–1260, Jul. 2009.
10. Takahashi, Y., K. Yamada, and T. Abe, "Examination of radio frequency blackout for an inflatable vehicle during atmospheric reentry," *Journal of Spacecraft and Rockets*, Vol. 51, No. 2, 1954–1964, Mar. 2014.
11. Kim, M., M. Keidar, and I. D. Boyd, "Analysis of an electromagnetic mitigation scheme for reentry telemetry through plasma," *Journal of Spacecraft and Rockets*, Vol. 45, No. 6, 1223–1229, Nov. 2008.
12. Shashurin, A., T. Zhuang, G. Teel, M. Keidar, M. Kundrapu, J. Loverich, I. I. Beilis, and Y. Raitses, "Laboratory modeling of the plasma layer at hypersonic flight," *Journal of Spacecraft and Rockets*, Vol. 51, No. 3, 838–845, May 2014.
13. Kundrapu, M., J. Loverich, K. Beckwith, P. Stoltz, A. Shashurin, and M. Keidar, "Modeling radio communication blackout and blackout mitigation in hypersonic vehicles," *Journal of Spacecraft and Rockets*, 1–10, 2015.
14. Gilllman, E. D., J. E. Foster, and I. M. Blankson, "Review of leading approaches for mitigating hypersonic vehicle communications blackout and a method of ceramic particulate injection via cathode spot arcs for blackout mitigation," NASA, Washington DC, NASA/TM-2010-216220, 2010.
15. Vilnrotter, V. A., S. Hinedi, and R. Kumar, "Frequency estimation techniques for high dynamic trajectories," *IEEE Transactions on Aerospace and Electronic Systems*, Vol. 25, No. 4, 559–577, Jul. 1989.
16. Hurd, W. J., P. Estabrook, C. S. Racho, and E. Satorius, "Critical spacecraft-to-earth communications for Mars exploration rover (MER) entry, descent and landing," *Proc. IEEE Aerospace Conference*, Vol. 3, 1283–1292, MT, Mar. 2002.

17. Satorius, E., P. Estabrook, J. Wilson, and D. Fort, "Direct-to-Earth communications and signal processing for Mars exploration rover entry, descent and landing," *The Interplanetary Network Progress Report, IPN Progress Report 42-153*, May 2003.
18. Soriano, M., S. Finley, D. Fort, B. Schratz, P. Ilott, R. Mukai, P. Estabrook, K. Oudrhiri, D. Kahan, and E. Satorius, "Direct-to-Earth communications with Mars science laboratory during entry, descent, and landing," *Proc. 2013 IEEE Aerospace Conference*, 1–14, 2013.
19. Cattivelli, F. S., P. Estabrook, E. H. Satorius, and A. H. Sayed, "Carrier recovery enhancement for maximum-likelihood doppler shift estimation in Mars exploration missions," *IEEE Journal of Selected Topics in Signal Processing*, Vol. 2, No. 5, 658–669, Oct. 2008.
20. Lopes, C. G., E. H. Satorius, P. Estabrook, and A. H. Sayed, "Adaptive carrier tracking for Mars to earth communications during entry, descent, and landing," *IEEE Transactions on Aerospace and Electronic Systems*, Vol. 46, No. 4, 1865–1879, Oct. 2010.
21. Chung, S. T. and A. J. Goldsmith, "Degrees of freedom in adaptive modulation: A unified view," *IEEE Transactions on Communications*, Vol. 49, No. 9, 1561–1571, Sep. 2001.
22. Goldsmith, A. J., *Wireless Communications*, Cambridge University Press, Cambridge, U.K., 2005.
23. Svensson, A., "An overview of adaptive modulation schemes for known and predicted channels," *Proceedings of the IEEE*, Vol. 95, No. 12, 2322–2336, Dec. 2007.
24. Yang, T. S., A. Duel-Hallen, and H. Hallen, "Reliable adaptive modulation aided by observations of another fading channel," *IEEE Transactions on Communications*, Vol. 52, No. 4, 605–611, Apr. 2004.
25. Duel-Hallen, A., S. Hu, and H. Hallen, "Long-range prediction of fading signals: Enabling adaptive transmission for mobile radio channels," *IEEE Signal Processing Magazine*, Vol. 17, No. 3, 62–75, May 2000.
26. Duel-Hallen, A., "Fading channel prediction for mobile radio adaptive transmission systems," *Proceedings of the IEEE*, Vol. 95, No. 12, 2299–2313, Dec. 2007.
27. Bachynski, M. P., T. W. Johnston, and I. Shkarofsky, "Electromagnetic properties of high temperature air," *Proceedings of the IRE*, Vol. 48, No. 3, 347–356, Mar. 1960.
28. He, G., Y. Zhan, N. Ge, Y. Pei, B. Wu, and Y. Zhao, "Channel characterization and finite-state Markov channel modeling for time-varying plasma sheath surrounding hypersonic vehicles," *Progress In Electromagnetic Research*, Vol. 145, 299–308, 2014.
29. He, G., Y. Zhan, N. Ge, Y. Pei, and B. Wu, "Measuring the time-varying channel characteristics of the plasma sheath from the reflected signal," *IEEE Transactions on Plasma Science*, Vol. 42, No. 12, 3975–3981, Dec. 2014.
30. Lin, T. C. and L. K. Sproul, "Influence of reentry turbulent plasma fluctuation on EM wave propagation," *Computers and Fluids*, Vol. 35, 703–711, 2006.
31. Demetriades, A. and R. Grabow, "Mean and fluctuating electron density in equilibrium turbulent boundary layers," *AIAA*, Vol. 9, 1533–1538, Aug. 1971.
32. Josyula, E. and W. Bailey, "Governing equations for weakly ionized plasma fields of aerospace vehicles," *Journal of Spacecraft and Rockets*, Vol. 40, No. 6, 845–857, Nov. 2003.
33. Kasdin, N. J., "Discrete simulation of colored noise and stochastic processes and $1/f^{\alpha}$ power law noise generation," *Proceedings of the IEEE*, Vol. 83, No. 5, 802–827, May 1995.
34. Orfanidis, S. J., *Electromagnetic Waves and Antennas*, Online Book, 1999.